

1 **Comparison of the multifractal characteristics of heavy**
2 **metals in soils within two areas of contrasting economic**
3 **activities in China**

4 Xiaohui Li^{a, b}, Xiangling Li^a, Feng Yuan^{a, b*}, Simon M. Jowitt^{c, d}, Taofa Zhou^a, Kui
5 Yang^a, Jie Zhou^a, Xunyu Hu^a, Yang Li^a

6 a. School of Resources and Environmental Engineering, Hefei University of
7 Technology, Hefei 230009, China

8 b. Xinjiang Research Centre for Mineral Resources, Xinjiang Institute of Ecology and
9 Geography, Chinese Academy of Sciences, Urumqi, Xinjiang 830011, China

10 c. School of Earth, Atmosphere and Environment, Monash University, Wellington
11 Road, Clayton, VIC 3800, Australia

12 d. Department of Geoscience, University of Nevada Las Vegas, 4505 S. Maryland
13 Parkway, Las Vegas, NV 89154-4010, USA

14 *Corresponding author: Email: yf_hfut@163.com, Tel: [+8605512901648](tel:+8605512901648)

15 **Abstract**

16 Industrial and agricultural activities can generate heavy metal pollution that can
17 cause a number of negative environmental and health impacts. This means that
18 evaluating heavy metal pollution and identifying the sources of these pollutants,
19 especially in urban or developed areas, is an important first step in mitigating the
20 effects of these contaminating but necessary economic activities. Here, we present the
21 results of a heavy metal (Cu, Pb, Zn, Cd, As and Hg) soil geochemical survey in Hefei
22 city. We used a multifractal spectral technique to identify and compare the
23 multifractality of heavy metal concentrations of soils within the industrial Daxing and
24 agricultural Yicheng areas. This paper uses three multifractal parameters ($\Delta\alpha$, $\Delta f(\alpha)$
25 and $\tau''(1)$) to indicate the overall amount of multifractality within the soil geochemical

26 data. The results show all of the elements barring Hg have larger $\Delta\alpha$, $\Delta f(\alpha)$ and $\tau''(1)$
27 values in the Daxing area compared to the Yicheng area. The degree of multifractality
28 suggests that the differing economic activities in Daxing and Yicheng generate very
29 different heavy metal pollution loads. In addition, the industrial Daxing area contains
30 significant Pb and Cd soil contamination, whereas Hg is the main heavy metal present
31 in soils within the Yicheng area, indicating that differing clean-up procedures and
32 approaches to remediating these polluted areas are needed. The results also indicate
33 that multifractal modeling and the associated generation of multifractal parameters
34 can be a useful approach in the evaluation of heavy metal pollution in soils.

35

36 **Keywords:** soil geochemistry; multifractal modelling; heavy metal pollution; Hefei

37

38 **1. Introduction and overview of the study area**

39 Heavy metal pollution within soil poses a serious risk for human health and the
40 environment, and thus soil pollution caused by anthropogenic activities (including
41 industry and agriculture) has been the focus of a significant amount of research (e.g.,
42 [Leyval et al., 1997](#); [Thomas and Stefan, 2002](#); [McGrath et al., 2004](#); [Wang et al., 2007](#);
43 [Luo et al., 2011](#)). Analyzing soil geochemistry and pollution using multifractal
44 techniques may allow for assessing many of the problems of nonlinear variability
45 which commonly arise when dealing with pollutants, as well as enabling the
46 identification of non-linear characteristics within datasets. This approach can yield
47 new information that can be used to understand the factors controlling the distribution
48 of key elements within the objects or data being studied ([Salvadori, 1997](#); [Gonçalves,](#)
49 [2000](#); [Zuo et al., 2012](#)). This in turn means that determining the multifractal
50 characteristics of the distribution of heavy metals in soils can improve our
51 understanding of any heavy metal pollution that is associated with these differing
52 anthropogenic activities.

53 Multifractal techniques include singularity mapping and multifractal
54 interpolation that enable more detailed analysis of the spatial distribution of heavy

55 metals, concentration-area modeling that can be used to define threshold values
56 between background (i.e. geological) and anthropogenic anomalies (Lima et al., 2003),
57 spectral density-area modeling that can be used to define thresholds to separate
58 anomalies (i.e., anthropogenically derived heavy metal concentrations in this case)
59 from background concentrations (i.e., geologically derived heavy metal
60 concentrations; Cheng, 2001), and multifractal spectra that highlights non-linear
61 characteristics and identifies anomalous behavior that reflects the characteristics of
62 some multifractal sets (Gonçalves, 2000; Albanese et al., 2007; Guillén et al., 2011),
63 such as the presence of porous structures and spatial variations in soil properties
64 (Caniego et al., 2005; Dathe et al., 2006). This means that multifractal techniques can
65 be useful tools for the analysis of heavy metal pollution within soils (e.g., Salvadori et
66 al., 1997; Lima et al., 2003; Albanese et al., 2007; Guillén et al., 2011). These
67 multifractal techniques are not only used in environmental science, but also in a
68 number of differing fields, including geophysics (Schertzer et al., 2011), medicine
69 (Jennane et al., 2001), computer science (Wendt et al., 2009), geology (Cheng, 1995;
70 Deng et al., 2011; Yuan et al., 2012, 2015) and ecology (Pascual et al., 1995), among
71 others.

72 Hefei is the capital of Anhui Province, China, and has an urban area that includes
73 the towns of Daxing and Yicheng, which focus on industrial and agricultural activities,
74 respectively. Here, we use multifractal spectra techniques and three parameters ($\Delta\alpha$,
75 $\Delta f(\alpha)$ and $\tau''(1)$) to analyze and compare the degree and characteristics of the
76 multifractality of heavy metal contamination in soils associated with anthropogenic
77 activities in this region. The results will further enable and inform future planning for
78 any necessary remediation of the soils in the Daxing and Yicheng areas.

79 **2. Study area and geochemical data**

80 **2.1 Study area**

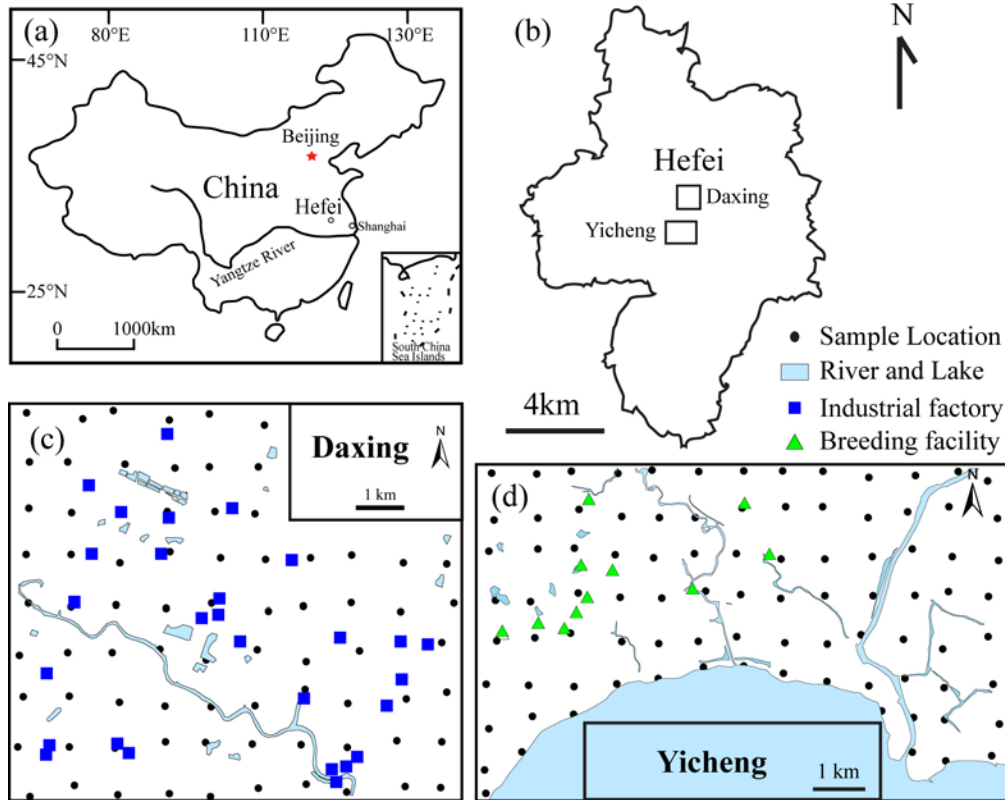
81 The city of Hefei is situated in central–eastern China (Fig. 1(a)), has
82 approximately 7.7 million inhabitants and covers an area of around 11,408 km². This
83 paper focuses on the towns of Daxing and Yicheng (Fig. 1(b)), with the former

84 representing one of the traditional industrial areas of Hefei and containing numerous
85 factories that are involved in the steel industry, chemical industry, paper making, and
86 the production of furniture and construction materials, among others. In contrast, the
87 town of Yicheng focuses its economic activities on agricultural production, byproduct
88 processing, livestock and poultry breeding, ornamentals, and other enterprises related
89 to agricultural activity.

90 **2.2 Sampling and analysis**

91 The study areas are covered by Quaternary sedimentary soils and are free of both
92 natural mineralization and mining-related contamination. A total of 169 surface (<20
93 cm depth) soil samples were taken from the towns of Daxing and Yicheng on 1 × 1
94 km grids, yielding 78 samples from Daxing and 91 samples from Yicheng (Fig.
95 1(c–d)). Sampling errors were minimized by splitting each sample into 3–5
96 sub-samples, each of which weighed more than 500 g. Each of these sub-samples was
97 air-dried before being broken up using a wooden roller and then sieved to pass
98 through a 0.85 mm mesh. The concentrations of 6 heavy metal elements (Cu, Pb, Zn,
99 Cd, As and Hg) were determined during this study, with Cd, Cu, Pb and Zn
100 concentrations determined by inductively coupled plasma–mass spectrometry
101 (ICP–MS), whereas Hg and As concentrations were determined by hydride
102 generation–atomic fluorescence spectrometry (AFS; Armstrong et al., 1999;
103 Gómez-Ariza et al., 2000). These techniques have detection limits of 1 ppm for Cu, 2
104 ppm for Pb and Zn, 30 ppb for Cd, 0.5 ppm for As and 5 ppb for Hg. The accuracy of
105 these data was monitored by repeat and replicate determinations using instrumental
106 neutron activation analysis (INAA), with analytical precision monitored using
107 variance of the results obtained from duplicate analyses.

108



109
110
111
112
113

Fig. 1. Location of Hefei in central-eastern China (a); location of the study areas within Hefei (b); the 1 × 1 km grids used for soil sampling in the towns of Daxing (c) and Yicheng (d)

114 3. Multifractal spectrum analysis

115 Multifractal formalisms can decompose self-similar measures into intertwined
 116 fractal sets that are characterized by singularity strength and fractal dimensions
 117 (Cheng, 1999). Using multifractal techniques allows non-linear characteristics within
 118 datasets to be identified, enabling the extraction of information that can be used to
 119 understand the factors controlling the distribution of key elements within the data.
 120 Fractal spectra ($f(\alpha)$) are formalisms that can be used to describe the multifractal
 121 characteristics of a dataset and can be estimated using box-counting based moment,
 122 gliding box, histogram and wavelet methods, among others (Cheng, 1999; Lopes and
 123 Betrouni, 2009). The most widely used of these methods are the box-counting and
 124 gliding box methods, both of which are based on the moment method.

125 The calculation of the mass exponent function $\tau(q)$ for the gliding box method is
 126 different from the box-counting method, with the gliding box method providing a

127 useful approach that can increase the number of samples that are available for
 128 statistical estimation within a dataset (Buczowski et al., 1998; Tarquis et al., 2006;
 129 Xie et al., 2010). This means that the gliding box approach often provides better
 130 results with lower uncertainties than the box-counting method (Cheng, 1999). As such,
 131 we have used the gliding box approach during this study. The calculation of the mass
 132 exponent function $\tau(q)$ for the gliding box method uses a partition function as follows
 133 (Cheng, 1999):

$$134 \quad \langle \tau(q) \rangle + D = \lim_{\varepsilon \rightarrow 0} \left(\frac{\log(\mu^q(\varepsilon))}{\log(\varepsilon)} \right) = \lim_{\varepsilon \rightarrow 0} \left(\frac{\log \left(\frac{1}{N^*(\varepsilon)} \sum_{i=1}^{N^*(\varepsilon)} \mu_i^q(\varepsilon) \right)}{\log(\varepsilon)} \right) \quad (1)$$

135 where $\mu_i(\varepsilon)$ denotes a measure with the i_{th} cell of a gliding box of size ε , q is the order
 136 moment of this measure (this paper used a range of q values from -10 to 10 with an
 137 interval of 1), $\langle \rangle$ indicates the statistical moment, and $N^*(\varepsilon)$ indicates the total
 138 number of gliding boxes of size ε with $\mu_i(\varepsilon)$ values different from 0 .

139 The values of $\tau(q)$ derived using this equation can be then used to determine
 140 singularity α and fractal spectra $f(\alpha)$ values using a Legendre transformation, as
 141 expressed below:

$$142 \quad \alpha(q) = \frac{d\tau(q)}{dq} \quad (2)$$

$$143 \quad f(\alpha) = q\alpha(q) - \tau(q) = q \frac{d\tau(q)}{dq} - \tau(q) \quad (3)$$

144 $\Delta\alpha$ and Δf are essential parameters required to analyze the multifractal
 145 characteristics of a given dataset. The widths of the left ($\Delta\alpha_L$) and right ($\Delta\alpha_R$) branches
 146 within the multifractal spectra are then defined using the following equations:

$$147 \quad \Delta\alpha_L = \alpha_0 - \alpha_{\min} \quad (4)$$

$$148 \quad \Delta\alpha_R = \alpha_{\max} - \alpha_0 \quad (5)$$

$$149 \quad \Delta\alpha = \alpha_{\max} - \alpha_{\min} \quad (6)$$

150 and the height difference $\Delta f(\alpha)$ between the two ends of the multifractal spectrum is

151 then extracted using:

$$152 \quad \Delta f(\alpha) = f(\alpha_{\max}) - f(\alpha_{\min}) \quad (7)$$

153 Higher $\Delta\alpha$ and $\Delta f(\alpha)$ values are generally indicative of datasets with more
154 heterogeneous patterns (ordered, complex, clustered) and higher levels of
155 multifractality (Cheng, 1999; Kravchenko et al., 1999). In addition, local
156 multifractality $\tau''(1)$, which may determined by ordinary spatial analysis functions
157 (autocorrelations and semivariograms), can also be used as a measure to quantitatively
158 characterize the multifractality of a dataset using equation 8 (Cheng, 2006):

$$159 \quad \tau''(1) = \tau(2) - 2\tau(1) + \tau(0) \quad (8)$$

160 If μ is a multifractal and $-D < \tau''(1) < 0$, where D is the gliding-box dimension,
161 then more negative values of $\tau''(1)$ are indicative of higher degrees of multifractality,
162 whereas otherwise $\tau''(1) = 0$ for monofractal.

163 **4. Geochemical analysis results**

164 A statistical summary of the soil geochemical data for the study area is given in
165 Table 1. Samples from the Daxing area have higher Cu, Pb, Zn, Cd and As maximum,
166 mean, standard deviation, skewness, and kurtosis values than soil samples from the
167 Yicheng area, whereas the Yicheng area has a higher maximum Hg concentration
168 value than the Daxing area. In addition, the soil samples from Daxing have much
169 higher coefficient of variation (CV) values for Cu, Pb, Zn, Cd and As than the
170 samples from the Yicheng area, indicating that soils in the Daxing area contain higher
171 and more variable concentrations of these elements. This also suggests that samples
172 from the Daxing area containing elevated concentrations of heavy metals were
173 probably contaminated by anthropogenic activity.

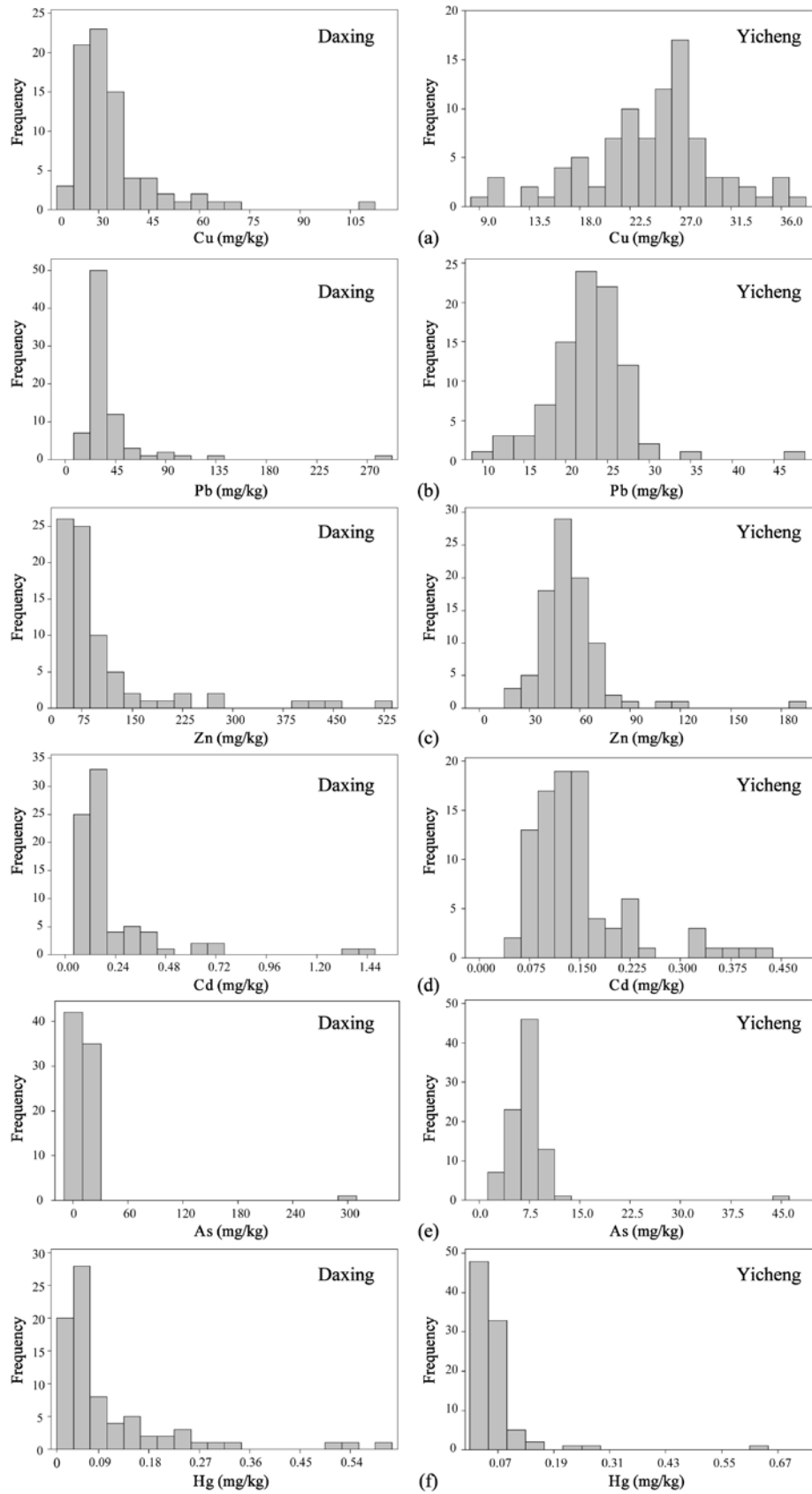
174 All of the elements (barring Pb and Cu in the Yicheng area) in both the Yicheng
175 and Daxing areas yielded concentration histograms that are positively skewed and
176 contain some outliers (Fig. 2), indicating that these data have non-normal and
177 potentially fractal- or multifractal-type distributions. This means that multifractal
178 techniques are highly suited for the characterization of the geochemistry of the soils.

179

180 Table 1. Summary statistics of soil heavy metal concentrations within samples from the Daxing
 181 and Yicheng areas.

Town	Element	Min	Max	Mean	Standard deviation	Skewness	Kurtosis	CV*
		(mg/kg)	(mg/kg)	(mg/kg)	-	-	-	(%)
Daxing	Cu	19.00	111.50	33.87	13.26	3.20	14.93	39.16
	Pb	18.90	291.30	39.57	35.03	5.37	35.41	88.51
	Zn	40.90	526.10	105.8	94.40	2.91	8.59	89.19
	Cd	0.045	1.48	0.23	0.24	3.45	13.81	108.23
	As	4.93	308.20	13.97	33.89	8.72	76.64	242.56
	Hg	0.03	0.60	0.11	0.11	2.68	7.78	107.29
Yicheng	Cu	9.60	37.80	24.34	5.77	-0.38	0.41	23.71
	Pb	10.40	46.30	22.77	4.91	0.87	5.51	21.56
	Zn	20.80	194.80	54.70	21.43	3.45	20.27	39.17
	Cd	0.054	0.43	0.15	0.08	1.84	3.49	51.85
	As	2.30	44.20	7.29	4.39	6.68	56.55	60.24
	Hg	0.02	0.62	0.06	0.07	5.75	41.26	113.09

182 *CV: coefficient of variation.



183

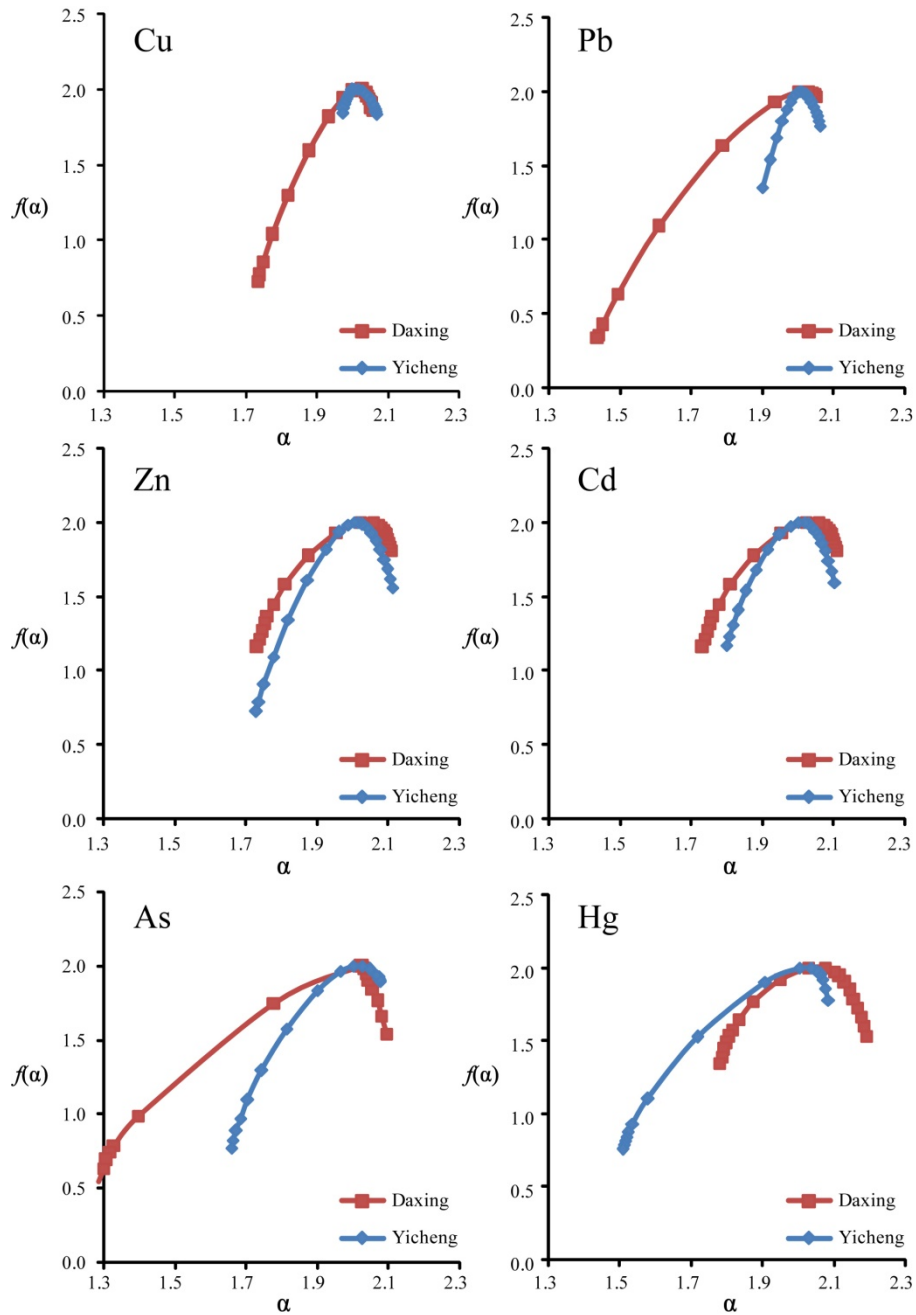
184 **Fig. 2.** Histograms showing the distribution of Cu (a), Pb (b), Zn (c), Cd (d), As (e) and Hg (f)
 185 concentrations within soils from the towns of Daxing and Yicheng.

186

187 **5. Calculation processes of multifractal spectrum and discussion**

188 The multifractal spectra (in the form of an α - $f(\alpha)$ diagram) for the geochemical
 189 data are shown in Fig. 3.

190



191

192 **Fig. 3.** Multifractal spectra ($f(\alpha)$ vs α) of the soil geochemical data from the Daxing and Yichen
 193 area.

194

195 These multifractal spectra have inverse bell shapes (Fig. 3) and are asymmetric
 196 (i.e. $\Delta\alpha_L$ values significantly differ from $\Delta\alpha_R$, equations 5-6) with the exception of the

197 Cu data for soils from the Yicheng area, indicating that the samples containing low
 198 and high concentrations of these elements are not evenly distributed within the study
 199 area (as is expected for areas containing point source pollutants like factories or
 200 animal breeding facilities).

201 The multifractal results given in Table 2 indicate that all of the elements (barring
 202 Cu and Pb in the Yicheng area) are characterized by a wide range of α values with
 203 $\tau''(1)$ values less than -0.01 and $\Delta f(\alpha)$ values larger than 0.5 , all of which indicate that
 204 these elements have a high multifractality within the soils in these two areas. All of
 205 the elements analyzed during this study (barring Hg) have higher $\Delta f(\alpha)$ and α values
 206 (except Zn) and lower $\tau''(1)$ values in soils from the Daxing area, with Hg having
 207 higher $\Delta f(\alpha)$ and $\Delta\alpha$ and lower $\tau''(1)$ values in soils from the Yicheng area (Table 2).
 208 This suggests that the industrial activities in the Daxing area generate multi-element
 209 heavy metal soil contamination, whereas the most significant heavy metal pollution
 210 associated with the agricultural activity in the Yicheng area is Hg contamination. The
 211 $\Delta f(\alpha)$ and $\Delta\alpha$ values of Hg in the Yicheng area are larger than the values for all other
 212 elements in this area as well as some of the elements in the Daxing area, indicating
 213 both the prevalence and significant degree of agricultural Hg contamination in the
 214 Yicheng area, even considering the lower overall concentrations of Hg within the
 215 Yicheng area compared to the Daxing area. This contamination should be considered
 216 a priority in terms of remediation, because the interaction between the agricultural
 217 activity in the Yicheng area and this Hg pollution could seriously impact human
 218 health, as Hg is preferentially concentrated upward in the food chain (e.g. (Jiang et al.,
 219 2006)). This means that although contamination in both areas needs to be evaluated
 220 further and should be remediated to avoid any deleterious effects, the fact that the Hg
 221 contamination in the Yicheng area may be more bioavailable and may have a larger
 222 effect on the population of this region (as a result of the agricultural activity in this
 223 area) means it should be considered a priority.

224

225 **Table 2.** Multifractal parameters of the elements analyzed during this study.

Town	Element	α_{\min}	α_{\max}	$\Delta\alpha_L$	$\Delta\alpha_R$	$\Delta\alpha$	$\Delta f(\alpha)$	$\tau''(1)$
------	---------	-----------------	-----------------	------------------	------------------	----------------	--------------------	-------------

Daxing	Cu	1.733	2.057	0.280	0.044	0.324	1.270	-0.015
	Pb	1.439	2.050	0.567	0.044	0.611	1.659	-0.068
	Zn	1.733	2.109	0.288	0.088	0.376	0.841	-0.066
	Cd	1.482	2.285	0.499	0.304	0.803	1.358	-0.066
	As	1.285	2.094	0.739	0.070	0.809	1.490	-0.243
	Hg	1.780	2.191	0.248	0.163	0.411	0.656	-0.079
Yicheng	Cu	1.971	2.067	0.036	0.060	0.096	0.168	-0.007
	Pb	1.900	2.062	0.104	0.058	0.162	0.646	-0.005
	Zn	1.729	2.112	0.275	0.108	0.383	1.275	-0.016
	Cd	1.800	2.103	0.201	0.102	0.303	0.829	-0.023
	As	1.659	2.076	0.343	0.075	0.418	1.224	-0.036
	Hg	1.507	2.084	0.497	0.080	0.577	1.243	-0.096

226

227 In order to compare variations in multifractality, the elements within the samples
228 from Daxing and Yicheng area were sorted by $\Delta\alpha$, $\Delta f(\alpha)$ and $\tau''(1)$ parameters,
229 respectively, in addition to sorting by coefficient of variation values (Table 3). The
230 data shown in Table 3 indicates that the Pb data within the Daxing area has close to
231 the lowest coefficient of variation, but largest the $\Delta f(\alpha)$ and $\tau''(1)$ values for these Pb
232 data are indicative of strongest multifractality compared to the other heavy metals in
233 the soils within the Daxing area. In comparison, the As data for soils in the Daxing
234 area yielded the largest coefficient of variation but the moderate $\Delta f(\alpha)$ and $\tau''(1)$
235 values, indicating these As data only have moderate multifractality. These differences
236 indicate that the multifractal parameters reveal new information about the nonlinear
237 variability and the characteristics of these geochemical data compared to the basic
238 statistics for these samples. In addition, the data given in Table 3 indicates that these
239 elements have different orders depending on whether they are sorted by $\Delta\alpha$, $\Delta f(\alpha)$ or
240 by $\tau''(1)$ values, all of which reflects differing aspects of the multifractality of these
241 data. Here we consider that $\Delta\alpha$, $\Delta f(\alpha)$ or by $\tau''(1)$ have equal weightings that reflect
242 the overall multifractality of the data from the study area. As such, the ordering of
243 these elements by $\Delta\alpha$, $\Delta f(\alpha)$ or by $\tau''(1)$ involved the summation of these values with
244 the summed ordering then sorted again to compare the overall multifractality of these
245 data.

246

247

Table 3. Elements sorted by multifractal parameters and basic statistic indices.

Town	Element	Order				
		Basic statistics	Multifractal parameters			
		Coefficient of variation	$\Delta\alpha$	$\Delta f(\alpha)$	$\tau''(1)$	Overall*
Daxing	Cu	6	6	4	6	6
	Pb	5	3	1	1	1
	Zn	4	5	5	2	4
	Cd	2	2	3	3	2
	As	1	1	2	5	3
	Hg	3	4	6	4	5
Yicheng	Cu	5	6	6	5	6
	Pb	6	5	5	6	5
	Zn	4	3	1	4	3
	Cd	3	4	4	3	4
	As	2	2	3	2	2
	Hg	1	1	2	1	1

248 Overall: the overall order of $\Delta\alpha$, $\Delta f(\alpha)$ and $\tau''(1)$.

249

250 The overall amount of multifractality within the soil geochemical data for the
 251 Daxing area decreases as follows: Pb>Cd>As>Zn>Hg>Cu, whereas the overall
 252 amount of multifractality within the soil geochemical data for the Yicheng area
 253 decreases as follows: Hg>As>Zn>Cd>Pb>Cu. The overall orders indicate that the Pb
 254 and Hg soil data have the highest degree of multifractality in the Daxing and Yicheng
 255 areas, respectively, whereas Cu has the weakest multifractality irrespective of the
 256 area.

257 We further analyzed the spatial distribution of contamination within soils from
 258 the Daxing and Yicheng areas and evaluated whether there is any significant
 259 correlation between multifractality and anthropogenic activity. Filled contour maps
 260 showing the distribution of Pb in the Daxing area and Hg and Cu in the Yicheng area
 261 were calculated using inverse distance weighted interpolation (Fig. 4–6). These
 262 figures show that areas with elevated levels of Pb contamination within the Daxing
 263 area are correlated with the location of industrial factories, although interestingly the
 264 areas in the upper and lower left hand side of Fig. 4 contain factories but not elevated
 265 concentrations of Pb. This indicates that the Pb concentrations in these soils may be
 266 dependent on both the presence and type of industry in this area, with some industries

267 polluting more than others, either as a direct result of the differing industries present
268 in this area or as a result of differing (or a lack of in some areas) approaches to
269 lessening environmental impacts. In comparison, the Hg contamination in the Yicheng
270 area is definitely spatially correlated with the location of agricultural breeding
271 facilities. Although the mean concentrations of Hg in soils are greater in the Daxing
272 area, all of the multifractal parameters determined during this study ($\Delta\alpha$, $\Delta f(\alpha)$ and
273 $\tau''(1)$) indicate that the Hg data in the Daxing area has a lower multifractality than
274 the Hg data in the Yicheng area. The Yicheng area is heavily agricultural, meaning
275 that the agricultural activities in this area may be both concentrating Hg as well as
276 contaminating soils. In addition, although the mean concentrations of Hg in the
277 Yicheng area are lower than in the soils in the Daxing area, the former has a higher
278 maximum concentration than the latter, and both areas have significant Hg
279 contamination. Indeed, the contamination in the Yicheng area may be of more concern
280 than the contamination in the Daxing area, as the agricultural activity in the Yicheng
281 area may lead to greater human intake of Hg than from the soils in the mainly
282 industrial Daxing area, a factor that could lead to serious health issues (e.g. Minamata
283 disease) caused by the potential concentration of Hg up the food chain. This indicates
284 that soils in both areas may well require control and remediation.

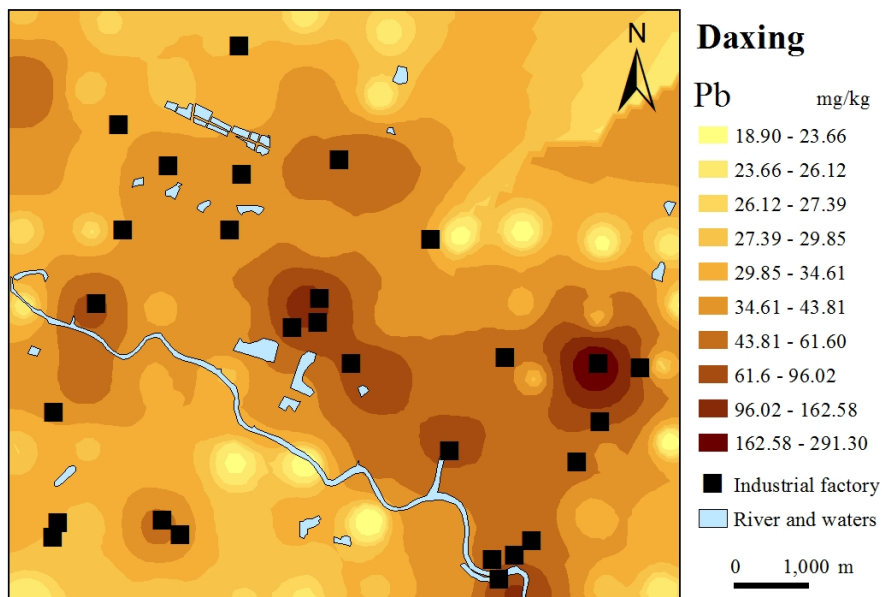
285 This distribution of soils with elevated concentrations of Hg also contrasts with
286 the symmetrical distribution and weakest multifractality for Cu within the Yicheng
287 area (Fig. 3, 5-6). Here, we generated a correlation matrix that compares the
288 relationship between the spatial density of breeding locations in the Yicheng area (Fig.
289 7) and filled contours maps showing the distribution of Hg (Fig. 5) and Cu (Fig. 6) in
290 this region to identify whether there are any spatial correlations between the location
291 of agricultural facilities and areas containing soils with elevated heavy metal
292 concentrations (Table 4). The correlation matrix shows a significant correlation
293 between agricultural facilities and high concentrations of Hg (coefficient of
294 correlation = 0.434), whereas the location of these agricultural breeding facilities and
295 areas of high Cu concentrations either have no relationship or are negatively
296 correlated (coefficient of correlation = -0.064). This indicates that very little Cu has

297 been anthropogenically added (or removed) from the soils in the Yicheng area,
298 suggesting that these soils may contain only natural background concentrations of Cu
299 and that the breeding facilities in this area do not produce significant Cu
300 contamination. The negative correlation coefficient, symmetrical distribution and
301 weakest multifractality of Cu give one clue to the spatial relationship between Cu
302 contamination and the river in the right hand side of Fig. 6. This may suggest a
303 non-anthropogenic source (e.g. flooding causing the deposition of Cu or some other
304 relationship between water and Cu contamination) for some of the slightly elevated
305 Cu concentrations in this region. In addition, the fact that some breeding facilities are
306 not associated with significant Hg contamination (Fig. 5) suggests again that although
307 there is a relationship between the presence of these facilities and contamination, it
308 may be that the Hg contamination in this area reflects differing types of breeding
309 facilities or differing (or a lack of) approaches to lessening environmental impacts.

310 These results indicate that multifractal modeling and the associated generation of
311 multifractal parameters are a useful approach in the evaluation of heavy metal
312 pollution in soils and the identification of major element of heavy metal
313 contamination. In addition, the differing orders of the multifractality of the
314 geochemical data for soils within the Daxing area and Yicheng area are indicative of a
315 significant difference in the geochemical characteristics (and heavy metal pollution)
316 in the soils within these two areas. This indicates that differing treatment strategy and
317 clean-up approaches to remediating these two polluted areas are needed, rather than a
318 single cover-all strategy and approach to the remediation of heavy metal pollution. A
319 significant number of different remediation approaches can be used to resolve the
320 issues of heavy metal soil contamination (e.g., Bech et al., 2014; Koptsik, 2014).
321 Although somewhat beyond the scope of this study, the multi-element nature of the
322 contamination in the Daxing area means that physical and chemical approaches to
323 remediation (i.e., soil removal, soil vitrification, soil consolidation, electroremediation,
324 or soil washing) are probably well suited for the remediation of heavy metal
325 contaminated soil in this region (especially Pb). In comparison, the differing (i.e.
326 Hg-dominated) type of soil contamination in the Yicheng area could be more

327 efficiently treated using microremediation and phytoremediation, primarily as the
 328 agriculture in this area requires a rapid reduction in the mobility and biological
 329 availability of heavy metals in the soils (Mulligan et al., 2001; Wang et al., 2006). In
 330 addition, the source of the Hg contamination (e.g. fertilizer, fodder, pesticides, water)
 331 remains unclear. Identifying this source is also beyond the scope of this paper
 332 although it is also clearly an area for future research, as the identification of the source
 333 or sources of this contamination may prevent the future heavy metal pollution of soils
 334 in this region.

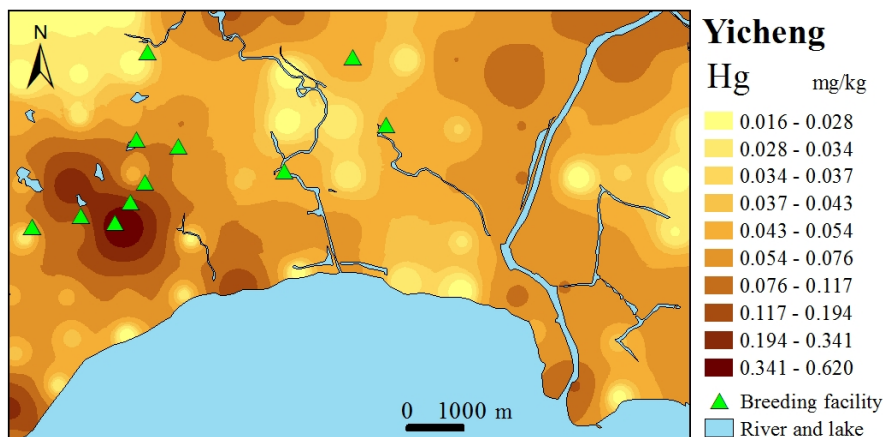
335



336

337 **Fig. 4.** Filled contour map generated by inverse distance weighted interpolation showing the
 338 spatial distribution of soil Pb concentrations in the Daxing area (generated using Inverse Distance
 339 Weighted Interpolation method within spatial analyst tools of the ArcGIS software package).

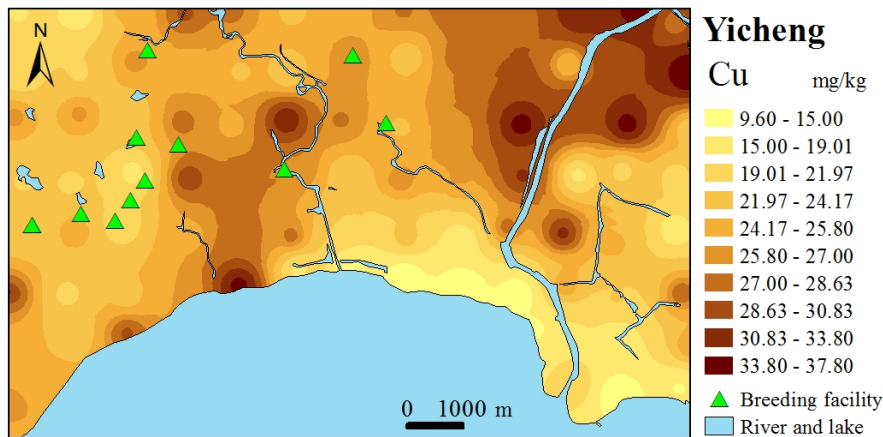
340



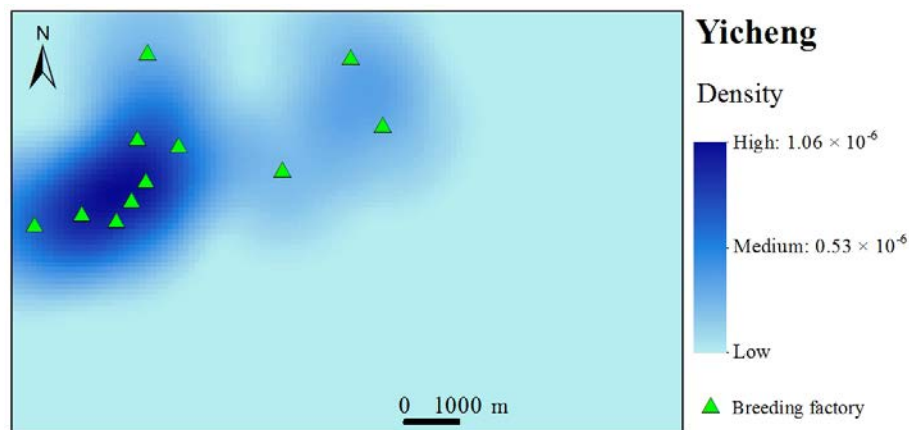
341

342 **Fig. 5.** Filled contour map generated by inverse distance weighted interpolation showing the

343 spatial distribution of soil Hg concentrations in the Yicheng area (generated using Inverse
 344 Distance Weighted Interpolation method within spatial analyst tools of the ArcGIS software
 345 package).
 346



347
 348 **Fig. 6.** Filled contour map generated by inverse distance weighted interpolation showing the
 349 spatial distribution of soil Cu concentrations and the location of breeding facilities in the Yicheng
 350 area (generated using Inverse Distance Weighted Interpolation method within spatial analyst tools
 351 of the ArcGIS software package).
 352



353
 354 **Fig. 7.** Density map of breeding facilities in Yicheng area (generated using the Kernel
 355 Density method within spatial analyst tools of the ArcGIS software package).
 356

357 **Table 4.** Correlation matrix comparing the breeding facility density map and the filled
 358 contour maps for Hg and Cu data for the Yicheng area (calculated using the Band
 359 Collection Statistics within spatial analyst tools of the ArcGIS software package).

Layers	Layer 1	Layer 2	Layer 3
Layer 1	1.000	0.434	-0.064
Layer 2	0.434	1.000	-0.464
Layer 3	-0.064	-0.464	1.000

360 Layer 1: Density map of breeding factories of Yicheng area (Fig. 7);
 361 Layer 2: Filled contour map of Hg concentrations of Yicheng area (Fig. 5);
 362 Layer 3: Filled contour map of Cu concentrations of Yicheng area (Fig. 6).

363

364 **5. Conclusions**

365 Multifractal modelling and the resulting multifractal parameters in this paper
366 indicate that the soils from the Daxing area have stronger multifractality for Cu, Pb,
367 Zn, Cd and As than soils from the Yicheng area, although the latter have relatively
368 strong multifractality for Hg. The ordering of values for the multifractal parameters
369 $\Delta\alpha$, $\Delta f(\alpha)$ and $\tau''(1)$ indicate the degree of multifractality for the geochemical data for
370 soils within the Daxing area descends as follows: Pb>Cd>As>Zn>Hg>Cu, whereas
371 within the Yicheng area descends as follows: Hg>As>Zn>Cd>Pb>Cu. In addition, Cu
372 concentrations in soils in the Yicheng area may still have their original (i.e. natural)
373 distribution and may not have been influenced by human activities. These data
374 indicate that the industrial activity concentrated in the Daxing area generates
375 multi-element heavy metal soil contamination whereas the agricultural activity
376 concentrated in the Yicheng area generates Hg-dominated heavy metal soil
377 contamination. The latter is important, as Hg contamination can cause serious health
378 issues (e.g. Minamata disease) and the soils in this area may require remediation,
379 especially as Hg can be concentrated up the food chain and the Yicheng area is
380 heavily agricultural, indicating that this activity may both be concentrating Hg as well
381 as contaminating soils in this area.

382 The results presented here indicate that multifractal modeling can be a useful
383 approach in the evaluation of heavy metal pollution in soils and the identification of
384 problematic heavy metals that need remediation in the research area.

385 **Acknowledgements**

386 This research was financially supported by funds from the China Academy of
387 Science "Light of West China" Program, the Fundamental Research Funds for the
388 Central Universities, and the Programme for New Century Excellent Talents in
389 University (Grant No. NCET-10-0324).

390 **References**

391 Albanese, S., De Vivo, B., Lima, A., and Cicchella, D.: Geochemical background and

392 baseline values of toxic elements in stream sediments of Campania region (Italy),
393 Journal of Geochemical Exploration, 93, 21-34, 2007.

394 Armstrong, H. E. L., Corns, W. T., Stockwell, P. B., O'Connor, G., Ebdon, L., and
395 Evans, E. H.: Comparison of afs and icp-ms detection coupled with gas
396 chromatography for the determination of methylmercury in marine
397 samples. *Analytica Chimica Acta*, 390, 245-253, 1999.

398 Bech, J., Korobova, E., Abreu, M., Bini, C., Chon, H. T., and Pérez-Sirvent, C.: Soil
399 pollution and reclamation, *Journal of Geochemical Exploration*, 147, 77-79, 2014.

400 Buczkowski, S., Hildgen, P., and Cartilier, L.: Measurements of fractal dimension by
401 box-counting: a critical analysis of data scatter, *Physica A Statistical Mechanics &
402 Its Applications*, 252, 23–34, 1998.

403 Caniego, F. J., Espejo, R., Martín, M. A., and José, F. S.: Multifractal scaling of soil
404 spatial variability, *Ecological Modelling*, 182, 291-303, 2005.

405 Cheng, Q.: The perimeter-area fractal model and its application to geology,
406 *Mathematical Geology*, 27, 69-82, 1995.

407 Cheng, Q.: The gliding box method for multifractal modeling, *Computer &
408 Geosciences*, 25, 1073-1079, 1999.

409 Cheng, Q.: Selection of Multifractal Scaling Breaks and Separation of Geochemical
410 and Geophysical Anomaly, *Journal of China University of Geosciences*, 1, 54-59,
411 2001.

412 Cheng, Q.: Multifractal modelling and spectrum analysis: Methods and applications to
413 gamma ray spectrometer data from southwestern Nova Scotia, Canada, *Science in
414 China Series D: Earth Sciences*, 49, 283-294, 2006.

415 Dathe, A., Tarquis, A. M., and Perrier, E.: Multifractal analysis of the pore- and
416 solid-phases in binary two-dimensional images of natural porous structures,
417 *Geoderma*, 134, 318–326, 2006.

418 Deng, J., Wang, Q., Wan, L., Liu, H., Yang, L., and Zhang, J.: A multifractal analysis
419 of mineralization characteristics of the Dayingezhuang disseminated-veinlet gold
420 deposit in the Jiaodong gold province of China, *Ore Geology Reviews*, 40, 54–64,
421 2011.

422 Gómez-Ariza, J. L., Sánchez-Rodas, D., Giráldez, I., and Morales, E.: A comparison
423 between ICP-MS and AFS detection for arsenic speciation in environmental
424 samples, *Talanta*, 51, 257-268, 2000.

425 Gonçalves, M. A.: Characterization of Geochemical Distributions Using Multifractal
426 Models, *Mathematical Geology*, 33, 41-61, 2000.

427 Guillén, M. T., Delgado, J., Albanese, S., Nieto, J. M., Lima, A., and De Vivo, B.:
428 Environmental geochemical mapping of Huelva municipality soils (SW Spain) as
429 a tool to determine background and baseline values, *Journal of Geochemical*
430 *Exploration*, 109, 59-69, 2011.

431 Jennane, R., Ohley, W. J., Majumdar, S., and Lemineur, G.: Fractal analysis of bone
432 X-ray tomographic microscopy projections, *IEEE Transactions on Medical*
433 *Imaging*, 20, 443-449, 2001.

434 Jiang, G. B., Shi, J. B., and Feng, X. B.: Mercury Pollution in China, *Environmental*
435 *Science & Technology*, 40, 3672-3678, 2006.

436 Koptsik, G. N.: Modern approaches to remediation of heavy metal polluted soils: A
437 review, *Eurasian Soil Science*, 47, 707-722, 2014.

438 Kravchenko, A., Boast, C., and Bullock, D.: Multifractal analysis of soil spatial
439 variability, *Agronomy Journal*, 91, 1033-1041, 1999.

440 Leyval, C., Turnau, K., and Haselwandter, K.: Effect of heavy metal pollution on
441 mycorrhizal colonization and function: physiological, ecological and applied
442 aspects, *Mycorrhiza*, 7, 139-153, 1997.

443 Lima, A., De Vivo, B., Cicchella, D., Cortini, M., and Albanese, S.: Multifractal IDW
444 interpolation and fractal filtering method in environmental studies: an application
445 on regional stream sediments of (Italy), Campania region, *Applied Geochemistry*,
446 18, 1853-1865, 2003.

447 Lopes, R., and Betrouni, N.: Fractal and multifractal analysis: A review, *Medical*
448 *Image Analysis*, 13, 634-649, 2009.

449 Luo, C., Liu, C., Yan, W., Xiang, L., Li, F., Gan, Z., and Li, X.: Heavy metal
450 contamination in soils and vegetables near an e-waste processing site, South
451 China, *Journal of Hazardous Materials*, 186, 481-490, 2011.

452 McGrath, D., Zhang, C., and Carton, O. T.: Geostatistical analyses and hazard
453 assessment on soil lead in Silvermines area, Ireland, *Environmental Pollution*,
454 127, 239-248, 2004.

455 Mulligan, C., Yong, R., and Gibbs, B. F.: Remediation technologies for
456 metal-contaminated soils and groundwater: an evaluation. *Engineering Geology*,
457 60, 193-207, 2001,

458 Pascual, M., Ascioti, F., and Caswell, H.: Intermittency in the plankton: a multifractal
459 analysis of zooplankton biomass variability, *Journal of Plankton Research*, 17,
460 167-168, 1995.

461 Salvadori, G., Ratti, S. P., and Belli, G.: Fractal and multifractal approach to
462 environmental pollution, *Environmental Science & Pollution Research*, 4, 91-98,
463 1997.

464 Schertzer, D., Lovejoy, S., Schmitt, F., Chigirinskaya, Y., and Marsan, D.: Multifractal
465 Cascade Dynamics and Turbulent Intermittency, *Fractals-complex Geometry*
466 *Patterns & Scaling in Nature & Society*, 5, 427-471, 2011.

467 Tarquis, A. M., McInnes, K. J., Key, J. R., Saa, A., García, M. R., and Díaz, M. C.:
468 Multiscaling analysis in a structured clay soil using 2D images, *Journal of*
469 *Hydrology*, 322, 236-246, 2006.

470 Thomas, K., and Stefan, S.: Estimate of heavy metal contamination in soils after a
471 mining accident using reflectance spectroscopy, *Environmental Science &*
472 *Technology*, 36, 2742-2747, 2002.

473 Wang, Y., and Greger, M.: Use of iodide to enhance the phytoextraction of
474 mercury-contaminated soil. *Science of the Total Environment*, 368, 30-39, 2006.

475 Wang, Y. P., Shi, J. Y., Wang, H., Lin, Q., Chen, X. C., and Chen, Y. X.: The influence
476 of soil heavy metals pollution on soil microbial biomass, enzyme activity, and
477 community composition near a copper smelter. *Ecotox Environ Safe*,
478 *Ecotoxicology & Environmental Safety*, 67, 75-81, 2007.

479 Wendt, H., Roux, S. G., Jaffard, S., and Abry, P.: Wavelet leaders and bootstrap for
480 multifractal analysis of images, *Signal Processing*, 89, 1100–1114, 2009.

481 Xie, S., Cheng, Q., Xing, X., Bao, Z., and Chen, Z.: Geochemical multifractal

482 distribution patterns in sediments from ordered streams, *Geoderma*, 160, 36-46,
483 2010.

484 Yuan, F., Li, X., Jowitt, S. M., Zhang, M., Jia, C., Bai, X., and Zhou, T.: Anomaly
485 identification in soil geochemistry using multifractal interpolation: A case study
486 using the distribution of Cu and Au in soils from the Tongling mining district,
487 Yangtze metallogenic belt, Anhui province, China, *Journal of Geochemical*
488 *Exploration*, 116-117, 28-39, 2012.

489 Yuan, F., Li, X., Zhou, T., Deng, Y., Zhang, D., Xu, C., Zhang, R., Jia, C., and Jowitt,
490 S. M.: Multifractal modelling-based mapping and identification of geochemical
491 anomalies associated with Cu and Au mineralisation in the NW Junggar area of
492 northern Xinjiang Province, China, *Journal of Geochemical Exploration*, 154,
493 252-264, 2015.

494 Zuo, R., Carranza, E. J. M., and Cheng, Q.: Fractal/multifractal modelling of
495 geochemical exploration data, *Journal of Geochemical Exploration*, 122, 1-3,
496 2012.